

Low-Temperature Heat Capacity of a Superconducting Alloy of Aluminum*

F. A. OTTER† AND D. E. MAPOTHER

University of Illinois, Urbana, Illinois

(Received October 9, 1961)

The specific heat of a precipitation-hardening alloy of aluminum (Alcoa 6063) has been measured down to 1.8°K in both the annealed and hardened conditions. From 1.8° to 4.2°K, the data for both conditions are well represented by $C = \gamma T + 1.944 \times 10^6 (T/\theta_D)^3$ mjoule/mole-deg with $\gamma = 1.33 \pm 0.02$ mjoule/mole-deg² and $\theta_D = 430 \pm 4^\circ\text{K}$ for the annealed condition. In this temperature range, both γ and θ_D increase for the alloy in the hardened condition. The changes are $d\gamma/\gamma = 1.1 \pm 0.5$ percent and $d\theta_D/\theta_D = 1.3 \pm 0.6\%$. No change in θ_D was observed from 10° to 20°K. The change in θ_D is quantitatively consistent with previous work on the shift of the superconducting critical field curve of this alloy with hardening. Both the present change in θ_D and the previously reported shift in H_c indicate an internal compressive stress in the fully hardened alloy which is believed to arise from coherency stress in the early stages of precipitation. The observed change in γ seems inconclusive with respect to the coherency stress hypothesis for reasons which are discussed.

INTRODUCTION

A PREVIOUS study^{1,2} of the effect of precipitation hardening on the superconducting properties of an aluminum alloy (Alcoa 6063) has shown that the critical field curves for the alloy in the annealed (fully precipitated) and in the quenched conditions are essentially the same as that of pure aluminum. The H_c curve for the fully hardened condition is shifted to lower fields. The shift was expressed as

$$\Delta H_c = H_c(\text{Hard}) - H_c(\text{Al}) = -9.450 + 0.04617 H_c(\text{Al}), \quad (1)$$

with H_c in gauss. This gives a shift in the critical temperature of

$$\Delta T_c/T_c = (-4.6 \pm 0.1)\% \quad (2)$$

in going from the annealed to the fully hardened condition.

The present experiment was designed to measure the variation of the heat capacity with hardening in the same alloy to establish the correlation with the critical field results. A simple argument based on the early Fröhlich-Bardeen theory^{3,4} indicated that $\Delta\theta_D/\theta_D = -\Delta T_c/T_c$ and thus predicted an easily measurable $\Delta\theta_D$ with hardening.¹ Such a large increase in θ_D was not found although at the lowest temperatures the data show small increases in both θ_D and the normal electronic specific heat constant γ .

The subsequent appearance of the Bardeen-Cooper-Schrieffer (BCS) theory⁵ clarified the inadequacy of

the original simple theory; in particular its implicit assumption that ΔT_c could be explained solely in terms of changes in the lattice properties as reflected by $\Delta\theta_D$. The BCS theory shows T_c to be proportional to the product $\theta_D \exp[-1/N(0)V]$ where $N(0)$ is the density of states at the Fermi level and V is the electron-electron interaction potential. All of the parameters, θ_D , $N(0)$, and V are sensitive to stress and the electronic effects associated with $N(0)V$ can exceed those due to lattice changes and reflected in θ_D . However, there are difficulties in making quantitative application of the BCS theory to the present alloy since our experiments indicate that the Al lattice is inhomogeneous on a microscopic scale.

It appears that the superconductivity changes associated with precipitation hardening are due to coherency stress around the Guinier-Preston (G.P.) zones in early stages of precipitation hardening.² The changes observed in θ_D and γ are discussed in terms of this interpretation.

APPARATUS AND EXPERIMENTAL PROCEDURE

A. Cooling Curve Method

The heat capacity was determined by a procedure which is an adaptation of the cooling curve method described by Logan, Clement, and Jeffers.⁶ The sample is mounted so that the only important thermal contact with the liquid helium bath is a small and measurable heat leak through the electrical leads to the specimen. If the temperature T of the sample is above bath temperature, then the sample tends to cool slowly to bath temperature. At a temperature T the heat capacity C is given by

$$CdT/dt = C\dot{T} = -\dot{Q}_0, \quad (3)$$

where t is the time and \dot{Q}_0 is the rate at which heat leaves the specimen. The time rate of change of temperature \dot{T} is measured during the cooling. The heat leak down the leads (\dot{Q}_0) is found from a separate measurement.

* J. K. Logan, J. R. Clement, and H. R. Jeffers, Phys. Rev. **105**, 1435 (1957).

* This work received partial support from the U. S. Army Research Office (Durham) and is based on a thesis submitted to the University of Illinois by F. A. Otter in partial fulfillment of the requirements for the Ph.D. degree.

† Present Address: Ohio University, Athens, Ohio.

¹ R. E. Mould and D. E. Mapother, Phys. Rev. **96**, 797 (1953), also R. E. Mould, Ph.D. thesis, University of Illinois, Urbana, Illinois, 1954 (unpublished).

² R. E. Mould and D. E. Mapother, Phys. Rev. **125**, 33 (1962).

³ H. Fröhlich, Phys. Rev. **79**, 845 (1950); Proc. Phys. Soc. (London) **A64**, 129 (1951).

⁴ P. M. Marcus, Phys. Rev. **91**, 216 (1953).

⁵ J. Bardeen, L. N. Cooper, and J. R. Schrieffer, Phys. Rev. **108**, 1175 (1957). For a recent discussion in the context of stress effects see M. Garfinkel and D. E. Mapother, Phys. Rev. **122**, 459 (1961).

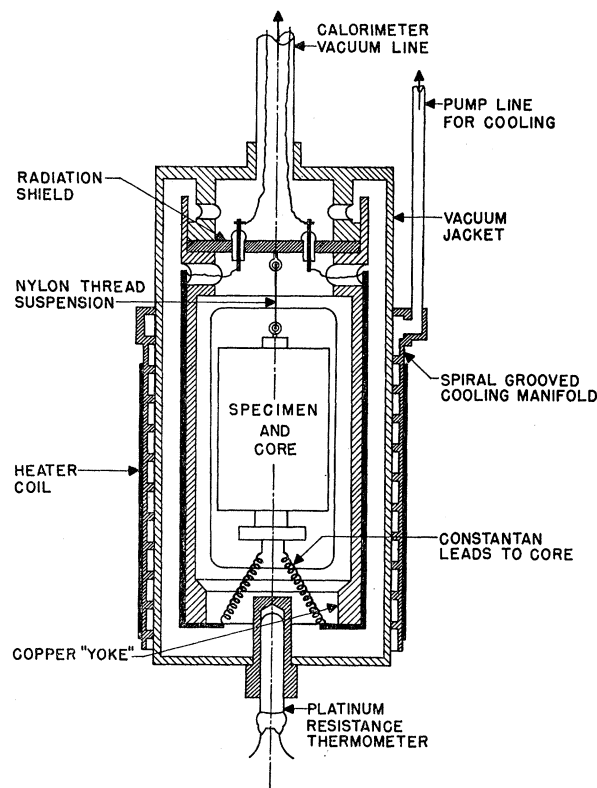


FIG. 1. Schematic view of the calorimeter can. The "yoke" is a copper cylinder with two large windows milled on opposite sides for access to the specimen. Dark lines along both sides of the yoke indicate heavy copper electrical leads cemented and clamped to the yoke for thermal grounding. (The glass insulated bushings in the radiation shield are also used for thermal grounding and do not support a vacuum.)

By dissipating power in the specimen via an electrical heater, one can hold T constant at any desired value above bath temperature simply by adjusting the current through the heater. This power \dot{Q}_c (called cancellation power hereafter) is measured to give \dot{Q}_0 ($\dot{Q}_c = \dot{Q}_0$ if $\dot{T} = 0$). Combining \dot{Q}_0 and T in Eq. (3) then gives C .

B. Cryostat and Sample Mounting

Figure 1 is a schematic view of the calorimeter can. The purpose of the yoke is to support the leads and to keep them in thermal contact with the liquid helium bath. Figure 2 shows the tapered core containing a $\frac{1}{2}$ watt, 38 ohm Allen-Bradley carbon resistor and a manganin heater. The core is made largely of Alcoa 6063 aluminum and is used interchangeably with several specimens. A matching taper on the inside of the specimens provides support for the specimens and helps to improve thermal contact between the core and the sample. The electrical leads from the bottom of the core provided some mechanical support to the core and also the desired heat leak to the helium bath. For measurements above 4°K, seven No. 30 constantan

leads 8.6 cm long were used, and the same leads cut to 2 cm length were used below 4°K. The heat capacity of the core is about 0.1 to 0.2 that of the specimens used and was determined in separate runs with no specimen mounted.

The temperature of the calorimeter assembly may be stabilized at values above 4.2°K by allowing the liquid helium level in the surrounding Dewar to fall below the bottom of the can. Cooling is then adjusted by the rate at which helium vapor from the liquid bath is pumped through the spiral manifold on the vacuum can. The temperature of the assembly is automatically regulated by controlling the power to the heater coil.

C. Measuring Circuits and Techniques

Many of the measuring circuits used in this work are essentially the same as those used by Logan *et al.*⁶ except for minor details. The resistance of the carbon-resistance thermometer was continuously monitored by a Wheatstone bridge network with the cooling curves appearing as strip chart records of resistance R vs time t , giving \dot{R} . From the temperature calibration of the carbon resistor, one obtains

$$\dot{T} = \dot{R}(dT/dR). \quad (4)$$

The cancellation power \dot{Q}_c was measured by potentiometric means.

In the interest of speed, reliability, and convenience, cooling rate data were also recorded by use of a Robot Star camera mounted in front of the panel containing the bridge decades and a Standard Electric model S-10 clock. A photocell arrangement was used to trip the camera as the bridge passed balance thus photographing the bridge setting and the clock reading at which balance occurred. The film record of R vs t was then easily read on a film viewer at a great saving in time, in comparison with the effort required to get an accurate time record from the strip chart.

The carbon resistor was calibrated in the range 1.2° to 4.2°K against the vapor pressure of the helium bath

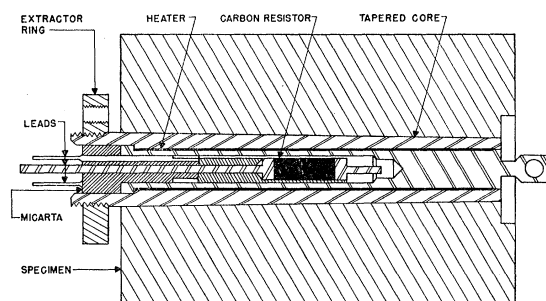


FIG. 2. Cross section view of the specimen and heater core. The extractor ring permits forcible removal of the core from the specimen if the taper sticks.

using T_{55E} scale⁷ and making corrections for the hydrostatic head of helium.⁸ A platinum resistance thermometer calibrated by the National Bureau of Standards was used as a standard from 10° to 20°K, and the range 4.2° to 10°K was interpolated. The usual technique of fitting the data to an analytical expression⁹

$$[(\log_{10} R/T)]^{\frac{1}{2}} = a + b \log_{10} R, \quad (5)$$

and then plotting a deviation plot was used to obtain both T and dT/dR at the cancellation temperatures.

D. Description of Specimens

All of the specimens were machined from Alcoa 6063 aluminum and ranged in mass from 50 to 90 g. An analysis by the Detroit Testing Laboratories, Inc., revealed the following impurities: 0.02 weight percent Cu, 0.17% Fe, less than 0.01% Mn, 0.27% Si, 0.69% Mg, and traces of Zn and Ti. The remainder was aluminum. Controlled precipitation of the Mg and Si in the form Mg_2Si produces marked changes in the mechanical properties of the alloy.¹⁰

The specimens were all heat treated in a closed furnace in an atmosphere of argon gas to prevent oxidation. The annealed specimens were held at 575°C for two days and then cooled at a rate of less than 9°C per hour. The hardened specimens were also held at 575°C and then quenched in ice water and stored in liquid nitrogen. Maximum hardness was obtained by reheating to 175°C for 21 hr. The hardness of each specimen was checked on a Tukon Tester to see if the desired properties had been obtained. The annealed specimens all had a Diamond Point Hardness (Vickers Number) close to 28, and the fully hardened specimens ranged from 80 to 95. Pure aluminum has a hardness of about 25 on this same scale.

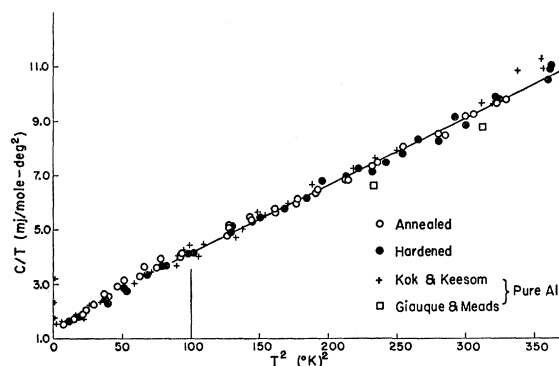


FIG. 3. Specific heat of Alcoa 6063 from 2° to 19°K.

⁷ J. R. Clement, J. K. Logan, and J. Gaffney, Phys. Rev. **100**, 743 (1955).

⁸ A discussion of the reliability of helium head corrections has been given by F. E. Hoare and J. E. Zimmerman, Rev. Sci. Instr. **30**, 184 (1959).

⁹ J. R. Clement and E. H. Quinell, Rev. Sci. Instr. **23**, 213 (1952).

¹⁰ J. A. Nock, Jr., Iron Age **159**, 48 (1947).

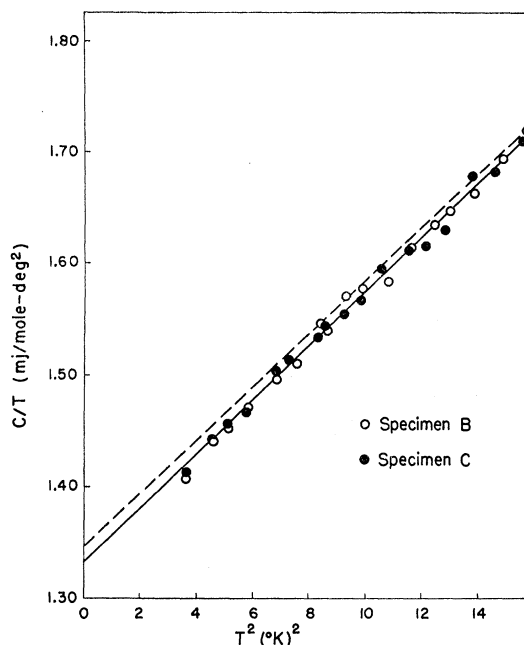


FIG. 4. Specific heat of annealed alloy specimens from 2 to 4°K. The dashed line corresponds to the hardened condition shown in Fig. 5.

EXPERIMENTAL RESULTS

A. Specific Heat Data

Figure 3 shows a plot of C/T vs T^2 in the temperature range 2° to 19°K. Figures 4 and 5 are similar plots for the range 2° to 4.2°K for annealed and fully hardened conditions, respectively. The data in the latter range can be well represented by the equation

$$C/T = \gamma + 1944T^2/\theta_D^3 \text{ joules/mol-deg}^2, \quad (6)$$

which gives a straight line on a plot like Fig. 4 or 5. The solid lines shown in Figs. 4 and 5 represent the least-squares fits to the data for the two conditions. The rms deviation of the data from each line is 0.4% for both cases. The constants of these lines are

$$\gamma = 1.33 \pm 0.02 \text{ mJoule/mol-deg}^2,$$

$$\theta_D = 430 \pm 4^\circ\text{K},$$

for the annealed condition and

$$\gamma = 1.35 \pm 0.02 \text{ mJoule/mol-deg}^2,$$

$$\theta_D = 436 \pm 4^\circ\text{K},$$

for the hardened condition. The curve for the hardened condition is also shown in Fig. 4 as a dashed line to show the comparison with the data for the annealed condition.

B. Comparison of Specimens

The limits of error in the constants given above include systematic uncertainties and are limits on the absolute values of the constants. All specimens were

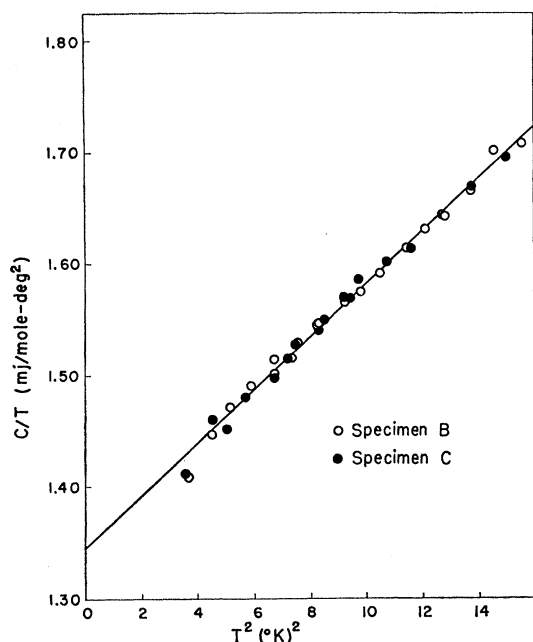


FIG. 5. Specific heat of hardened alloy specimens from 2 to 4°K.

measured with the same equipment under nearly identical conditions. For this reason, it is felt that the systematic errors should be about the same for all specimens, and the relative values of the constants should be known with somewhat less uncertainty than the absolute values. The changes observed going from the annealed to hard conditions are

$$d\theta_D/\theta_D = +(1.3 \pm 0.6)\%, \quad (7)$$

and

$$d\gamma/\gamma = +(1.1 \pm 0.5)\%.$$

Examination of Fig. 4 shows that the heat capacities in the two conditions are not very much different, and one might question whether the changes are really resolved. For this reason, measurements were made on two different sized specimens. The change in γ between the two sizes in the same condition was about 0.4% for both hardness conditions. The corresponding change in θ_D was about 0.6% for both conditions. The latter change is a reflection of the fact that the lattice contribution to C_v is small, and a small uncertainty in C_v corresponds to a large uncertainty in the lattice contribution.

In order to test the resolution of the θ_D 's a θ_D was calculated for each experimental point. This was done with the aid of Eq. (6) by subtracting off the electronic contribution to get

$$\theta_D^3 = 1944T^3/(C_v - \gamma T). \quad (8)$$

Figure 6 shows a plot of the number of values of θ_D falling in a given range of θ_D and it would appear that the θ_D 's for the two conditions are indeed resolved. In fact the resolution is likely to be better than the

TABLE I. Values of γ and θ_D for pure aluminum.

Investigator	γ (mjoule/mol-deg ²)	θ_D (°K)	Method ^a
Phillips ^b	1.35 ± 0.01	427.7 ± 1.0	A.C.
Howling <i>et al.</i> ^c	1.37 ± 0.05	408	T.W.
Zavaritskii ^d	1.27 ± 0.1	...	T.W.
Goodman ^e	1.40 ± 0.07	...	A.C.
Horton and Schiff ^f	...	428.1	...

^a The letters under "Method" refer to the experimental procedure used A.C.=adiabatic calorimetry and T.W.=temperature wave method.

^b N. E. Phillips, Phys. Rev. **114**, 676 (1959).

^c D. H. Howling, E. Mendoza, and J. E. Zimmerman, Proc. Roy. Soc. (London) **A229**, 86 (1955).

^d N. V. Zavaritskii, Soviet Phys.—JETP **7**, 773 (1958).

^e B. B. Goodman, Compt. rend. **244**, 2899 (1957).

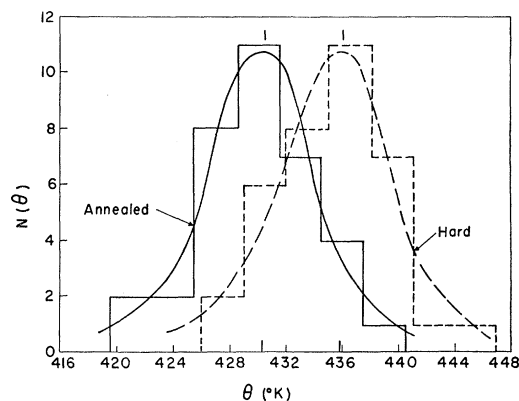
^f G. K. Horton and H. Schiff, Can. J. Phys. **36**, 1127 (1958); θ_D calculated from elastic constants reported by P. M. Sutton, Phys. Rev. **91**, 816 (1953).

figure would indicate because the procedure used essentially associates all the error in C_v with just the lattice contribution. Using the same technique, θ_D 's were also calculated up to 19°K, and a plot of θ_D vs T appears in Fig. 7.

The data for this alloy are in reasonably good agreement with previous heat capacity data for pure aluminum. Data of Keesom and Kok¹¹ and Giauque and Meads¹² are included in Fig. 3. Values of γ and θ_D found by various investigators are shown in Table I. The values of Phillips appear to be the most reliable of the published data.

DISCUSSION

The earlier superconducting measurements on this alloy have been interpreted as giving evidence of an effective internal compressive stress in the fully hardened condition.² This stress is conceived as an average of the microscopically varying coherency stress which arises in the early stages of precipitation of Mg and Si. In this interpretation the averaging is done by the superconducting electrons over distances com-

FIG. 6. Histogram showing the distribution of experimental values of θ_D for Alcoa 6063 in the low-temperature range (i.e., $T < 4.2^\circ\text{K}$).

¹¹ W. H. Keesom and J. A. Kok, Physica **4**, 835 (1937).

¹² W. F. Giauque and P. F. Meads, J. Am. Chem. Soc. **63**, 1897 (1941).

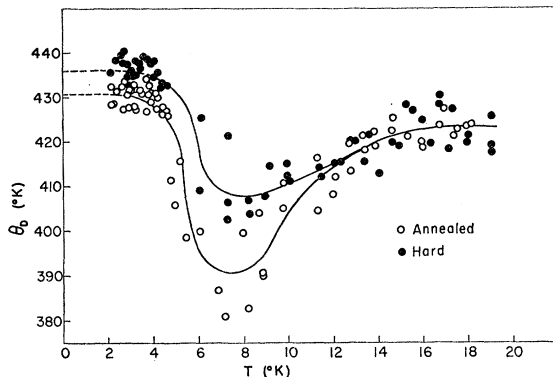


FIG. 7. Experimental values of Debye temperature for Alcoa 6063 over the full temperature range of these measurements.

parable with the range of order parameter¹³ ξ , which is a distance comparable to the dispersion of Guinier-Preston (G.P.) zones in the fully hardened condition.

The present calorimetric results on the shift in θ_D seem consistent with the foregoing interpretation. From the low-temperature value of $\Delta\theta_D$ a value may be calculated for the effective internal pressure from the relation

$$\Delta p = \Delta(\ln\theta_D)/k\Gamma = \Delta\theta_D/k\theta_D\Gamma. \quad (9)$$

In (9), Δp is the change in effective pressure resulting from the hardening process, k is the compressibility of Al, and Γ is the Grüneisen constant. The sense of the observed $\Delta\theta_D$ corresponds to a compression and thus agrees with the earlier results on the shift in H_c induced by hardening. Using the values¹⁴ $\Gamma=2.5$ and $k=1.2 \times 10^{-6} \text{ atm}^{-1}$,¹⁵ Eq. (9) gives $\Delta p=2.8 \times 10^8 \text{ atm}$ which is the same as the value estimated from the pressure effect on H_c according to the data of Muench.¹⁶

The apparent success of this calculation should not obscure the fact that it rests on some very elementary assumptions which, at present, cannot be regarded as experimentally well founded. In the absence of experimental data we have assumed that the bulk values of k and Γ can be applied to the long wavelength phonons which are dominant in θ_D at the lowest T values. Moreover, there seems to be some uncertainty¹⁴ about the true low-temperature value of Γ for Al and thus the numerical agreement may be fortuitous.

From 4.2° to 10°K the heat capacity of the annealed specimens appears to be greater than that of the hardened specimens. This trend represents a normal continuation of the results in the liquid helium range (where the present measurements are most accurate). However,

uncertainty in temperature extrapolation from 4.2° to 10°K prevents attaching much significance to this region.

Above 10°K the results (although less accurate than in the liquid helium range) indicate no difference in θ_D between the quenched and hardened conditions. If this is really true, the explanation may lie in a consideration of the dominant phonon wavelengths which contribute to the specific heat as the temperature falls. To estimate this, de Launay has given the expression¹⁷

$$\lambda_p T = 2a\theta_D/5, \quad (10)$$

where a is the lattice parameter and λ_p is the phonon wavelength at the peak in the energy distribution. For Al at the temperatures of 4°, 10°, and 20°K, Eq. (10) yields $\lambda_p=170, 70$, and 35 Å. Thus the dominant phonon wavelength at 10°K is about equal to the estimated dispersion of G.P. zones and the apparent disappearance of $\Delta\theta_D$ near 10°K may have its origin in a phonon diffraction effect.

We now turn to a consideration of the change observed in γ with hardening. As shown in Fig. 4 the data give an increase in γ with hardening. In view of the interpretation of the effect of hardening on H_c and θ_D it might seem reasonable to compare $\Delta\gamma$ with values for the volume derivative of γ for Al which are collected in Table II. To obtain a g value for the Al-Mg-Si alloy, the value of $d \ln v$ characteristic of the hardening process (where v is the molar volume) has been estimated from the Grüneisen relation (although, for reasons given below, the validity of this calculation for the alloy is dubious). This yields the value, $g=-2.1$, which, while of a reasonable order of magnitude, is anomalous in its algebraic sign. It is clear from Table II that the correct value of g for Al is subject to some uncertainty, but the negative value for the alloy seems more likely to reflect the inadequacy of the simplified assumptions of its calculation.

The problem which complicates the present interpretation (and, historically, has complicated all fundamental study of precipitation hardening) is the extremely fine scale of dispersion of the precipitating

TABLE II. Values of $g=d \ln \gamma/d \ln v$ for aluminum.

g	Method
$+2/3^a$	Free electron theory
$+1.4^{b,c}$	Thermal expansion
$+130^d$	Pressure effect on H_c
$+7^e$	Pressure effect on H_c

^a J. H. O. Varley, Proc. Roy. Soc. (London) **A237**, 413 (1956).

^b P. G. Klemens, Phys. Rev. **120**, 843 (1960).

^c G. K. White, *Proceedings of the Seventh International Conference on Low Temperature Physics* (University of Toronto Press, Toronto, 1961), pp. 685-687.

^d J. L. Olsen, Helv. Phys. Acta **32**, 310 (1959).

^e D. Gross and J. L. Olsen, Cryogenics **1**, 91 (1960).

¹³ T. E. Faber and A. B. Pippard, Proc. Roy. Soc. (London) **A231**, 336 (1955); also see *Progress in Low-Temperature Physics* (Interscience Publishers, Inc., New York, 1955), Vol. I, p. 159.

¹⁴ T. H. K. Barron, *Proceedings of the Seventh International Conference on Low-Temperature Physics* (University of Toronto Press, Toronto, 1961), pp. 661-664, and references cited there.

¹⁵ An average of values reported by P. M. Sutton, Phys. Rev. **91**, 816 (1953); and E. Goens, Ann. Physik **38**, 456 (1940).

¹⁶ N. L. Muench, Phys. Rev. **99**, 1814 (1955).

¹⁷ J. de Launay, *Solid-State Physics*, edited by F. Seitz and D. Turnbull (Academic Press Inc., New York, 1956), Vol. 2, p. 219.

aggregates.¹⁸ It is not clear what meaning to attach to the Δv associated with the hardening process. On one hand, both the ΔH_c and $\Delta\theta_D$ results indicate an effective compressive stress in the hardened alloy and thus, presumably, a decrease in the local value of v in the strained Al matrix. (From the Grüneisen relation, $\Delta v/v \simeq -0.3\%$ from both ΔH_c and $\Delta\theta_D$ data.) However, both x-ray and bulk-density measurements on this alloy show that its average lattice parameter does not differ from pure Al at any stage of precipitation by more than about 0.02%.¹⁹

These superficially contradictory results may be reconciled by considering the hardened alloy to consist of microscopic regions of Al matrix compressed by the finely dispersed regions in which the solute atoms collect. Unless future measurements show that the hardened alloy contracts more rapidly than the quenched alloy in cooling from 300° to 1°K,²⁰ it must be assumed that the volume shrinkage in the Al matrix due to coherency stress is cancelled by expansion in the volume of the G.P. zones. The ΔH_c and $\Delta\theta_D$ measurements and also the relatively small concentrations of Mg and Si in this alloy all indicate that the contracted Al matrix constitutes the major fraction of the macroscopic volume. Unfortunately the information available at present seems insufficient to give an unambiguous quantitative description of the local dimensions of either the strained Al matrix or the G.P. zones. Moreover the nature of γ (as well as the electronic band structure of normal Al) suggests that $\Delta\gamma$ could be sensitive to the microscopic distortion of the lattice around the G.P. zones.

Superficially it might appear that our values of the hardness induced changes ΔT_c , $\Delta\theta_D$, and $\Delta\gamma$ would permit the calculation of a hardness induced change in V , the electron-electron interaction potential of the BCS theory. However, the inhomogeneity within this alloy in the hardened state makes the application of the

BCS relation very questionable. It is doubtful that the change in θ_D seen at the lowest temperatures provides a reliable indication of the change in the region of the phonon spectrum which is important for the BCS interaction. Neither is it clear that the $\Delta\gamma$ value as averaged by the calorimetric measurement provides a valid estimate of the change in the density of states appropriate to the superconducting theory. For these reasons we think it would be premature to attempt an interpretation of the present results in terms of the BCS theory.

In conclusion, we find that the observed changes in θ_D are consistent with the hypothesis of coherency stress, originally suggested on the basis of ΔH_c data. However the corresponding changes in γ cannot be shown to bear a clear connection with this hypothesis. We suggest that this difference may be understood in terms of the effective range within the metal lattice which is sampled in the different phenomena. Thus the relatively long-range averaging of either superconducting electrons or low-temperature phonons primarily reflects conditions within the strained Al matrix which (on a volume basis) constitutes the greatest part of the specimen. On the other hand, the short-wavelength normal electrons near the Fermi surface of Al which determine γ may be substantially perturbed by the strong distortion of the lattice near the G.P. zones. In view of the present uncertainty about the physical situation, the $\Delta\gamma$ results are inconclusive with respect to the coherency stress hypothesis.

ACKNOWLEDGMENTS

We are indebted to J. R. Clement and J. K. Logan for valuable advice and assistance with the calorimetric techniques and also for allowing us to conduct preliminary experiments using their apparatus at the Naval Research Laboratories. One author (F.A.O.) received fellowship support from the U. S. Steel Foundation, Inc. The other (D.E.M.) is pleased to acknowledge the support of the J. S. Guggenheim Foundation and the cordial hospitality of the Physics Department of Cornell University during the final preparation of this manuscript.

¹⁸ A. H. Geisler and J. K. Hill, *Acta Cryst.* **1**, 238 (1948).

¹⁹ M. L. V. Gaylor and G. D. Preston, *J. Inst. Metals* **41**, 191 (1929). Alloy H_c of this work is close to the composition of Alcoa 6063.

²⁰ Preliminary measurements of thermal expansion from 300° to about 80°K show only a very small difference between this alloy in the quenched and fully hardened conditions.